12-2022

Femtosecond Pulse Filamentation in Dielectric Media Toward Photonics Sensor Fabrication

Anitha Narayanan
The University of Texas Rio Grande Valley

FEMTOSECOND PULSE FILAMENTATION IN DIELECTRIC MEDIA TOWARD PHOTONICS SENSOR FABRICATION

A Thesis

by

ANITHA NARAYANAN

Submitted in Partial Fulfillment of the

Requirements for the Degree of

MASTER OF SCIENCE IN ENGINEERING

Major Subject: Manufacturing Engineering

The University of Texas Rio Grande Valley

December 2022

FEMTOSECOND PULSE FILAMENTATION IN SAPPHIRE CRYSTALS TOWARD PHOTONICS SENSOR FABRICATION

A Thesis
by
ANITHA NARAYANAN

COMMITTEE MEMBERS

Dr. Farid Ahmed
Committee Chair

Dr. Jianzhi
Committee Member

Dr. Zhaohui Geng
Committee Member

December 2022

ABSTRACT

Narayanan, Anitha., Femtosecond Pulse Filamentation in Sapphire Crystals Toward Photonics Sensor Fabrication. Master of Science in Engineering (MSE), December, 2022, 52 pp., 5 tables, 30 figures, references, 44 titles.

Through pulse filamentation, femtosecond laser pulses have been utilized to modify the refractive indices of dielectric materials such as glass, A-plane sapphire crystal, and C-plane sapphire crystal. The 10x Infinity Corrected Lens was used, and the focusing condition was tuned as being the same and fixed to both glass and sapphire crystals. First, 8uJ of laser energy was optimized to produce controlled pulse filamentation voids in the glass. The laser intensity was then optimized to 2-3.5 uJ, 1.5 uJ, & 2.5 uJ, respectively, for the controlled pulse filamentation in A and C plane sapphire crystals. Due to the different crystal orientations in the A and C planes of sapphire, it was found that the morphology of pulse filamentary voids remains the same. The filament length extends as the laser energy rises for both the A and C planes, but the laser energy must be below a given threshold. The filamentation void length undergoes saturation after exceeding the threshold value. After successfully inducing controlled pulsed filamentation in both A and C-plane sapphire crystals, the parameters such as grating period, length of grating, etc. were optimized using the simulation program OPTIGRATING to construct sapphire optical fiber sensors.

DEDICATION

I will first and foremost dedicate this research to the omnipotent God who has given me the fortitude and wisdom to live a normal life. I sincerely dedicate my study to my family and friends. A special note of gratitude is extended to my loving parents, grandmother, Mrs. Komalam, Mr. Narayanan, and Mrs. Vellakutty, whose encouragement and call to perseverance have never left my ears. I would like to express my sincere gratitude to the Bhajan family for their unending love and support, in particular to Dr. Kusumam & Dr. Siddharthan, Dr. Palimar & Kavitha Palimar, Rajeswary Nair & Sunil Nair, Mili & Reghuraman, Maya Namboothiri & Hari Namboothiri, Dr. Nambiar and Sharmila Nambiar, and Hareendranath Vengilat & Aparna Hareendranath. I want to express my gratitude to Dr. Tina Thomas and Dr. Cheri Abraham for their unwavering support and encouragement. I dedicate this work to my best friends Anuja Giju, and Alex Ommen, who has been a constant source of inspiration to me. They have given me the motivation and discipline to approach a task with zeal and determination. Finally, I'd like to thank my coworkers and friends, without whom this project would not have been possible.

ACKNOWLEDGMENTS

The completion of this study could not have been possible without the expertise of Dr. Farid Ahmed, chair of my thesis committee, advisor, and professor. Dr. Ahmed has guided and mentored me tremendously throughout my thesis period with infinite patience. I will be eternally grateful to Dr. Jianzhi (James) Li for believing in me and providing me with the resources I needed to succeed. I'd also like to thank my colleagues and friends at the lab, especially Enrique and Ishrat, for making my time there so enjoyable. A special thanks to Shahriar Forhad for all of his support and for helping with the coding to control the devices. To my friend and brother-like Bala Murali Krishnan, I want to convey my gratitude for all of the moral support.

TABLE OF CONTENTS

LIST OF TABLES

LIST OF FIGURES

CHAPTER I

INTRODUCTION

As optical fiber sensors are safe, reliable, compact, lightweight, very sensitive, and suitable for use in harsh environments, there is a lot of research being done in this area right now. The most popular sensors on the market right now are constructed of silica, which has a melting point of roughly 1000 º C. There is a need for an optical fiber sensor that can resist high temperatures because several manufacturing processes, such Laser Powder Bed Fusion (LPBF), take place at extremely high temperatures (> 1000 º C). Since sapphire has a melting point of about 2053 º C, it makes an ideal option for this. Many issues in the manufacturing industries can be resolved by monitoring the processes like LPBF by incorporating them in LPBF if sapphire optical fiber sensors can be produced efficiently. Other than hard process monitoring like metallurgy, there will be applications in the areas of hypersonic weaponry and aviation.

Femtosecond laser material processing

Ultrashort pulsed lasers like picosecond and femtosecond lasers are helpful in fabricating optical and photonics devices in variety of fields. The femtosecond(fs) lasers are better that picosecond and nanosecond lasers, as its pulse duration is in the order of femtoseconds (10^{-15}), which is very less compared to the order of nanosecond (10^{-9}) and picoseconds (10^{-12}). The highly precise fs pulses are very efficient in many processes like milling, scribing, cutting, and drilling the hard& brittle materials with high tolerance and surface finish compared to the conventional machining processes. This thesis is mainly focused in processing the transparent dielectric

materials like glass and sapphire in making certain changes or perturbations in the bulk of the material. When a high peak optical power gets incident on the dielectric material, there comes the nonlinearity phenomena like Kerr effect, Pockels effect, self-phase modulation, multi-photon absorption etc. In this study, focus is mainly on the self-focusing property of the laser pulses inside the dielectric materials, to be precise, in making controlled damage inside the bulk of the materials to achieve a permanent refractive index change or a void. This can be achieved only through the spatial control in focusing the pulses and scanning the material with the optimized laser parameters.

Dielectric materials

The importance of dielectric materials lies in its property of dielectric polarization, ie the movement of positive and negatives charges along and opposite to the direction of electric field respectively under the influence of an applied electric field. The polarization is nothing, but the density of electric dipoles formed by the dielectric materials, when it is subjected to an external electric field. Electrical susceptibility is the property of dielectric materials or dielectric media, which determines the polarization, $P = \varepsilon_o \chi E$, where ε_o is the permittivity in free space, χ is the susceptibility and E is the electric field. The band gap of dielectrics is highly significant because of its substantial width, which explains why electromagnetic radiations of long wavelength can only excite electrons from the valence band to conduction band. The dielectrics for optical and photonics applications can be mainly divided into two categories: - Crystals & Glasses. The final goal of this study is to fabricate an optical fiber sensor made of a dielectric crystal for sensing applications in harsh environments.

Fiber optic sensing technology

An optical source, optical fiber, sensing element, or transducer to transform the measurand into an optical signal, optical detector, and processing electronics make up the fundamental parts of an optical fiber sensor system [Figure 1]. An optical fiber sensor is a system which functions by making use of different optical and electronic components altogether. The components in a standard optical fiber sensor system includes an optical source, a transducer or sensing element which is connected to the measurand, an optical detector and finally an electronic processing unit. Based on the variation in the properties of electromagnetic waves or light, optical fiber sensors can be utilized to sense a range of measurands, such as strain, temperature, refractive index, pressure, etc. The three primary categories of optical fiber sensing are intrinsic fiber sensing, extrinsic fiber sensing, and hybrid. Extrinsic sensing occurs when the optical fiber cable just serves as a communication link between the test end and an external sensor, i.e., the transducers are external to the fiber optic system. With intrinsic fiber sensing, a sensing element is built into or incorporated inside the fiber optic system, eliminating the need for coupling with external sensors. Hybrid sensors are just a combination of intrinsic and extrinsic sensors. Sensor's working principle is based on the modulations detected in the properties of light like intensity, wavelength or spectrum, phase, polarization, etc. while its passage through the fiber. [1].

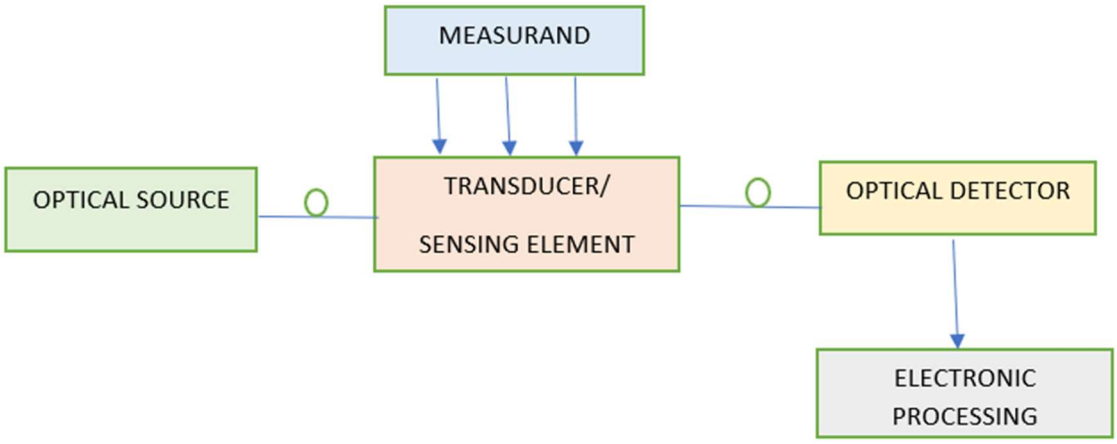

Figure 1:Fiber -optic system components[2]

In some sensors, the intensity of light will change after its passage through the sensing element, and these changes can be measured and compared to sense the value of parameters or measurand. Evanescent Field and Micro-bend sensors are two prominent examples of intensity-based sensors. While the bulk of light is transmitted through the optical fiber's core utilizing the phenomenon of total internal reflection, some light passes past the interface and enters the cladding with a lower refractive index. This electromagnetic field in the lower index region is known as Evanescent field, and it has an exponentially decreasing tendency. The interaction between the measurand and the evanescent field is the foundation of evanescent field sensor technology. For sensors based on Evanescent waves in the lower index range, chemical sensors provide the best illustration. The operation of a micro bend sensor is based on transmission loss, which results from the optical fiber's micro bending. The bending of a fiber results in structural changes with respect to the standard optical fiber, thereby changing

the angle of incident light in the core. The incident angle becomes greater than the critical angle, which will affect the total internal reflection (TIR) of light along the core. In other words, because of the leakage into the cladding caused by micro bending, the light intensity diminishes. So, by keeping an eye on and correlating the decline of light intensity, the measurand can be detected. Due to random variable losses in the sensing system (losses happening at the coupling, splice points etc.) intensity modulation-based sensors have a limited range of applications.

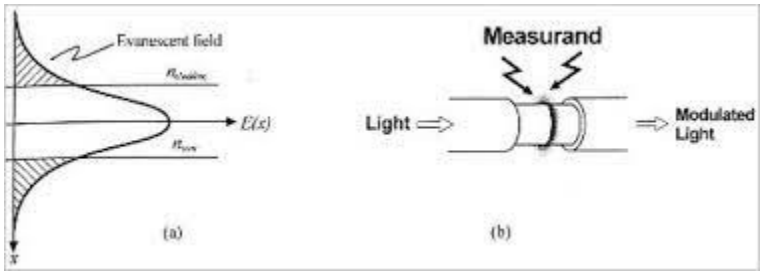

Figure 2 a) Evanescent Field in an optical fiber b) principle of Evanescent wave sensor[3]

In the case of wavelength modulation-based sensors, fluctuations in light's wavelength serve as the foundation for fiber sensing. The most common wavelength-based sensor is the Fiber Bragg Grating sensor. The Bragg Gratings (sensing elements) can be inscribed inside the core of the optical fiber using ultrashort lasers in UV and infrared region. Periodicity in the refractive index modulations acts as a filter in reflecting a particular wavelength and transmitting the rest of wavelengths. The reflected wavelength is known as the Bragg wavelength, which is represented by the notation λ_B. Any strain, temperature, or polarization change that affects the fiber's modal

index or grating pitch will produce a shift in the Bragg wavelength.

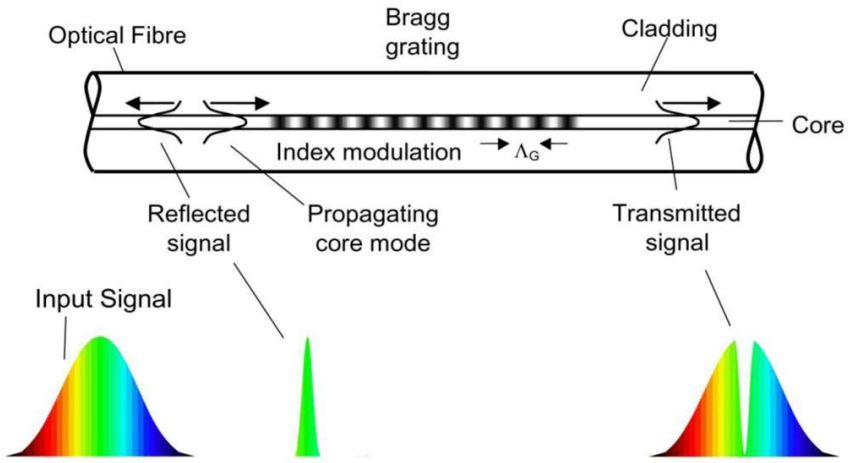

Figure 3: Working Principle of Fiber Bragg Grating Sensor[2]

In the case of polarization modulation Sensors, retarder or waveplate transmits light and changes the polarization state without any attenuation, deviation, or displacement of the beam. With regard to external disturbances, these fiber sensors function as a linear retarder and change the polarization of the light. Since the polarization state will vary depending on the perturbation, the change can be sensed. The prominent phase modulation sensors include Michelson, Mach Zehnder and Fabry Perot, which are the most often employed. An interferometer will split its incident light into two beams. One beam act as the reference and the other is exposed to the sensing environment. Despite coming from the same source, the light in both fibers is coherent and in phase. However, the sensor fiber will experience a phase shift due to changes in its environment that can be precisely quantified. Due to their small size, high-temperature sensitivity, and ambient

refractive index sensitivity, phase-based interferometric fiber optic sensors have received a great deal of interest. Fabry Perot Interferometer-based optical fiber sensor is the one that will be more useful in the manufacturing industries when compared to other examples of phase modulation sensors. A cavity with two parallel mirrors separated by a particular distance will act as a Fabry Perot Interferometer. The reflected and transmitted beam combines to form interference, and the sensing can be done based on the difference in interference patterns.

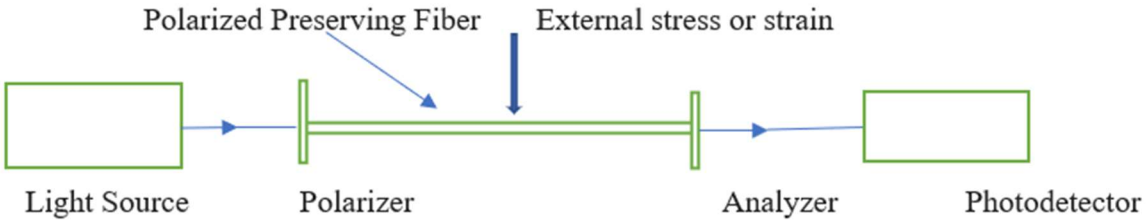

Figure 4: : Polarization-based optical fiber sensor system[2]

Significance of the problem

Femtosecond processing is useful for processing many dielectric materials to make its useful for optical and photonic applications. In particular, in optical materials with crystal structure, such as single crystal sapphire, it is exceedingly challenging to regulate the focusing conditions of lasers and tune laser parameters to generate the necessary structures or disturbances in dielectric media. Based on how the atoms are arranged in the lattice points, sapphire crystal planes can be classified as C-M-A-R. Varied planes have different damage thresholds, material

loss rates, and bonding energies between adjacent atomic levels. The plane that has been utilized the most is the C plane because it could provide a superior surface in less time than the other planes because of its high rate of material removal. A plane is very hard to process because of its high degree of scratch resistance and abrasive nature, hence no inventions with A plane sapphire for any device applications. It would be a very innovative and big accomplishment in the realm of laser machining and Manufacturing photonics if we could spatially manipulate the laser focus confinement and modify the laser parameters to process the A plane as this would open up new possibilities. The desired alteration that is attempting to be attained in this work is a modification of the refractive index for use in photonic sensors such as FBG sensors. The main difficulty to reach the goal of making Sapphire Fiber Bragg Grating (SFBG) sensors is to get controlled periodic damage or refractive index modulations to attain an efficient FBG. Until now, nobody has achieved 100% efficient SFBG, which is clear from the spectral response. The reflectivity achieved is very less, compared to FBG standard and the reflected Bragg peak is not prominent, which means the sensitivity won't be accurate. This difficulty in making standard FBG can be achieved by controlled pulse filamentation in the sapphire by spatially focusing the sample material using tight focusing conditions and optimized laser parameters.

Research questions

1) How do the femtosecond laser's conditions affect the refractive indices (RI) modifications in sapphire (A & C plane) crystals?

2) How does pulse energy impact the morphology (length & width) of the pulse filament-assisted RI change in sapphire crystals?

3) How do the crystal's A & C planes changes (if any) the morphology of the laser-written RI?

CHAPTER II

LITERATURE REVIEW

Materials

The only item that has been successful in the realm of optical fiber sensors is silica-based sensors. Most processes in the manufacturing sectors take place at extremely high temperatures, and silica optical fiber sensors lose their accuracy at these temperatures since it has a melting point between 1000 and 1400 degrees Celsius. To monitor every stage of industrial processes in tough settings, sensors that can endure high temperatures are required. Here, sapphire, which has a melting point of roughly 2053 degrees Celsius. Therefore, it will be very beneficial to tackle many difficulties in hostile environments if optical fiber sensors can be manufactured from single crystal sapphire. In this work, seeking to induce controlled laser damage in A & C planes of sapphire, which has not acquired so far. Researchers have already published articles on SFBG, but the spectral response and the sensitivity accuracy that they achieved is inadequate when compared to FBG standards. This has happened because they have not established the regulated refractive index modulations inside sapphire, as its exceedingly difficult to spatially control focus.

Femtosecond laser filamentation

The pulse filamentation is the equilibrium between Kerr self-focusing and plasma generated de-focusing by the laser pulses inside the dielectrics. When the femtosecond laser pulse gets struck on the dielectrics, it will start self-focusing inside the material, which will result in the ionization of that concentrated area. The ionization of the material will result in the loss of density at that location of the material, which permits the pulse to defocus to the nearby high-density

region. Once more, the Kerr effect will cause the laser pulse to begin self-focusing on the direction of the original laser path. This self-focusing and defocusing take place for many times until the intensity of the laser pulse is reduced, i.e., until the pulse filamentation gets weaker. The ultimate product is a pulse filamentary void or refractive index void[4]–[6].

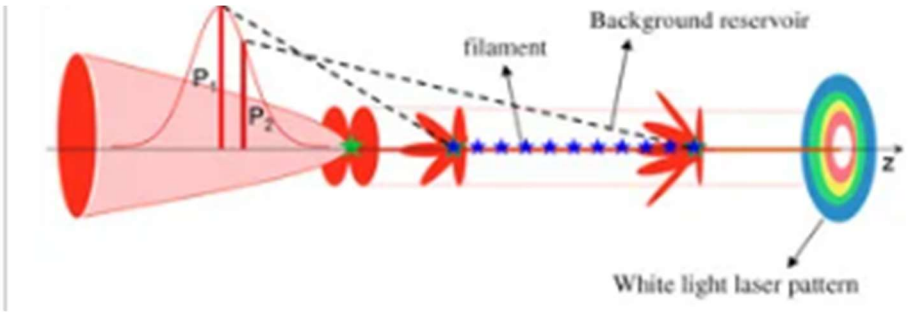

Figure 5: Schematic diagram of pulse filamentation[4]

Impact of focusing conditions

The laser power peak should be good enough to enhance the Kerr self-focusing effect on the sapphire crystal, but at the same time should not go above the threshold value to avoid uncontrolled laser damage. Controlled pulse filamentation is having lots of device applications like FBG inside the optical materials like sapphire crystal and amorphous glass. The main challenge is to acquire controlled pulse filamentation inside sapphire crystal, as its very difficult to achieve tight focusing or spatial confinement in focusing. The focusing conditions will be different for different materials as the energy gap to excite electrons to conduction band varies from material to material. So, need

to optimize focusing conditions separately for different materials, otherwise will result in an aperiodic pulse filamentary voids with different lengths and widths.

Dependence of laser parameters

Pulse Energy

The pulse energy needs to be below threshold for attaining the controlled pulse filamentation void with same morphology (filament length and width). The repeatability of filament morphology depends mainly on the pulse energy utilized to process sapphire crystal. The structure of the sapphire crystal will undergo perturbations based on the range of laser energy values. The modifications attained by the material can be divided into three based on the threshold values of pulse energy -: 1) Isotropic refractive index modulations (low intensity) 2) Anisotropic structure with Birefringence (intermediate intensity) 3) Cracks or Damage (high intensity). All these modifications take place due to different nonlinear phenomena, which will open up the way for new optical and photonics devices applications.

Repetition Rate (Pulse Picker Divider)

For controlled pulse filamentation to occur with the same morphology, the pulse energy must be below the threshold (filament length and width). The pulse energy used to cut the sapphire crystal determines in significant part how repeatably the filament shape changes. The range of laser energy values will cause changes in the sapphire crystal's structure. Based on the threshold values of the pulse energy, the alterations made to the material can be categorized into three categories: 1) Isotropic modulations of the refractive index (low intensity), 2) Anisotropic structure

with Birefringence (middle intensity), and 3) Cracks or Damage (high intensity). These changes are brought about by various nonlinear processes, which pave the way for new optical and photonics device applications.

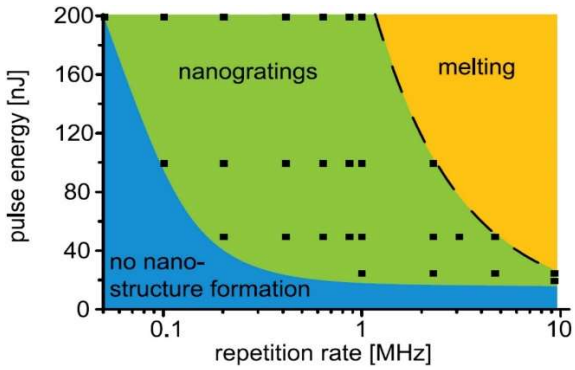

Figure 6 : Effects of repetition rate and pulse energy on silica glass[38]

Dependence of crystal orientation for processing sapphire

Figure [6] below depicts the crystal orientation of the sapphire crystal's A and C planes. The figure shows that compared to the C plane sapphire crystal, the A plane sapphire crystal required higher laser energy. In the vertical direction, there are four disk-like barriers that must be passed through in order to create pulse filaments. However, to write a refractive index void in the C plane crystal, only one disk-like structure must be penetrated. Determining the best laser settings and focusing circumstances based on the various crystals is therefore the key problem. It will be very challenging to process an A plane crystal because to its extremely high bonding energy between its atomic layers, limited rate of material removal, highly abrasive character, and high damage threshold. The average depth of refractive index lines on sapphire wafer rises with pulse energy and number, finally tending to be a saturation value.

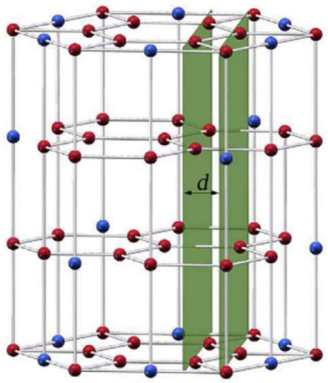

Figure 7: Crystal orientations of A plane sapphire[40]

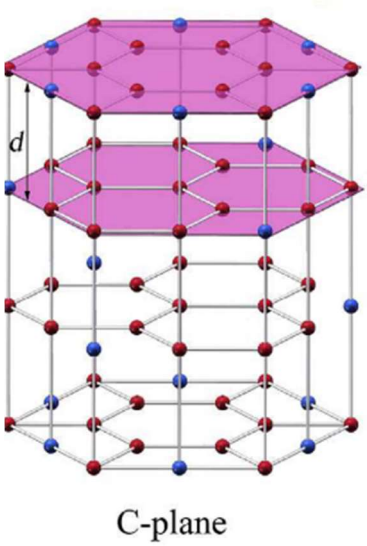

Figure 8:Crystal orientations of C plane sapphire[40]

CHAPTER III

METHODOLOGY

Materials

Glass

Figure 9: a) Glass wafer cut from the microscopic glass slide b) Daimond Cutter used to cut

Used a diamond cutter to create tiny glass wafers (Figure 9a) with dimensions of 10 mm in length and 5 mm in width from 1 mm thick microscopic glass slides. Glass has a melting point between 1400 and 1600 degrees Celsius, which is an amorphous solid. As sapphire is more expensive and glass is very cheap and user friendly, started with glass in order to get an idea in terms of focusing conditions and laser parameters needed for controlled pulse filamentation. Pulse filamentation can be used for variety of applications like cutting of glass without any gap, to create cracks or groove for the fabrication of Fabry Perot Interferometers, for achieve refractive index modifications to make FBG etc. Here in this study, experiments are designed in such a way to get refractive index voids inside the glass using the phenomenon of pulse filamentation. Already many

studies were published describing the nonlinear light matter interaction using ultrashort lasers and glass, but still some areas like the controlling the morphology of filamentary void has not explained well. The length and width of the filaments in glass depends on many factors like the laser parameters, focusing conditions, atomic structure of glass [**Figure 10**], mechanical and optical properties of glass etc. The glass will undergo bulk changes only when the laser energy is enough to move the electrons from valence band to conduction band. The intensity of electron density acts as a trigger for many nonlinear processes including avalanche ionization, Kerr effect etc. The relationship between density of electrons and the laser energy is shown in the below formula,

Equation 1

$$n = \frac{4\pi^2 \varepsilon m_c}{e^2} \nu^2$$

, where v is the laser frequency

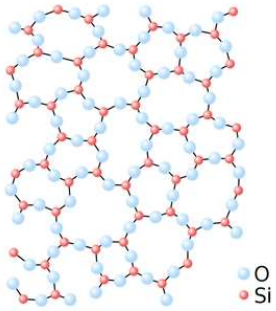

Figure: Atomic structure of Glass

A plane sapphire

There are some papers demonstrating the processing of sapphire crystal using femtosecond laser pulses, but never talked about the processing variations in different planes of sapphire. All

the time, the researchers just prefer to use C plane sapphire as the material for any sapphire-based experiments, never bothered about the effect of different crystal planes of sapphire in the morphology of pulse filamentation or any other features. There are mainly 4 different sapphire crystal planes: 1) C planes sapphire crystal, 2) M plane sapphire crystal, 3) A Plane sapphire crystal, 4) R plane sapphire crystal. Double side polished single crystal A plane sapphire wafers of 10 mm length, 5 mm of width and 0.5 mm of thickness from Advalue Technology LLC are used. A laser is used to cut a planar sapphire since they are too difficult to cut with a diamond cutter. Comparatively speaking to the C plane, A plane sapphire has a very high elastic modulus and is extremely hard and abrasive. Compared to the C plane, which has a low damage threshold, this wafer is more resistant to scratches with high damage threshold. Comparing to the C-M planes of sapphire, A plane sapphire is having the highest bonding energy between adjacent atomic layers. This material is viewed as being a poor choice for many applications due to all the aforementioned properties. One of my research questions is to find the difference in the processing of A & C plane sapphire, and thereafter to optimize the focusing conditions and laser parameters to process A plane sapphire, which will open up new possibilities. The electronic plasma dynamics and filament lifetimes varies from material to material based on their lattice arrangement of atoms. As there is difference in the crystal's structures of A & C planes of sapphire, without doubt there will be difference in the processing conditions also.

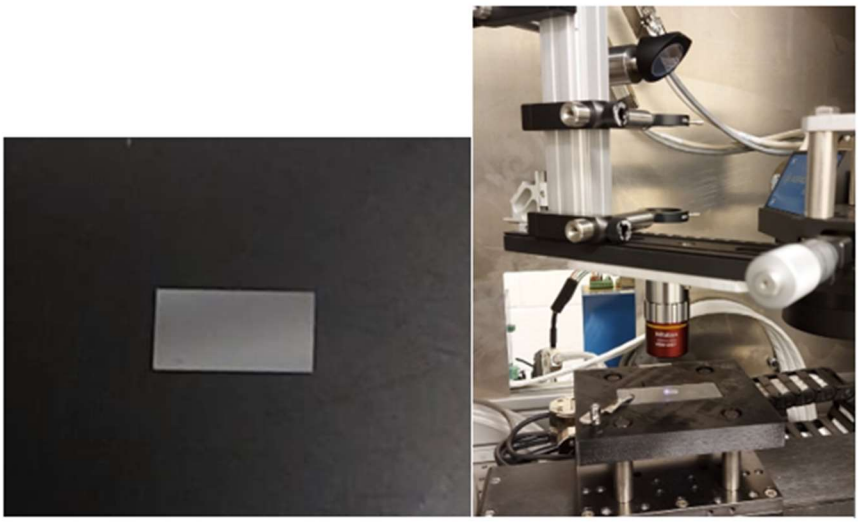

Figure 11: a) A plane sapphire of dimensions(10mmx5mmx0.5mm) b)Direct write on A plane sapphire wafer

C plane sapphire

The chemical formula for sapphire is Al_2O_3, with a rhombohedral structure. The linear and nonlinear refractive indices of the material are, $n_0 = 1.7717$ & $n_e = 1.76355$ respectively. Double side polished single crystal C plane sapphire wafers of 10 mm length, 5 mm of width and 0.5 mm of thickness from Advalue Technology LLC are used. C plane sapphire is regarded as a good material for a variety of applications because, when compared to A plane sapphire, it has a low damage threshold, a high rate of material removal, and a low bonding energy between neighboring atomic layers. The C plane of sapphire has a low elastic modulus and hardness value in comparison to other sapphire planes. Due to its rapid material removal rate, it is relatively simple to produce surfaces of superior quality in less time. Since multiphoton absorption and tunneling ionization are required for pulse filamentation, the laser energy should be sufficient to allow electrons to pass

across the C plane sapphire's large energy gap. The depth of laser focus also plays a role in triggering the self focusing, and thereafter to attain the controlled pulse filamentation. The figure below depicts a C plane sapphire being scanned by a femtosecond laser to create a refractive index void [Figure 12].

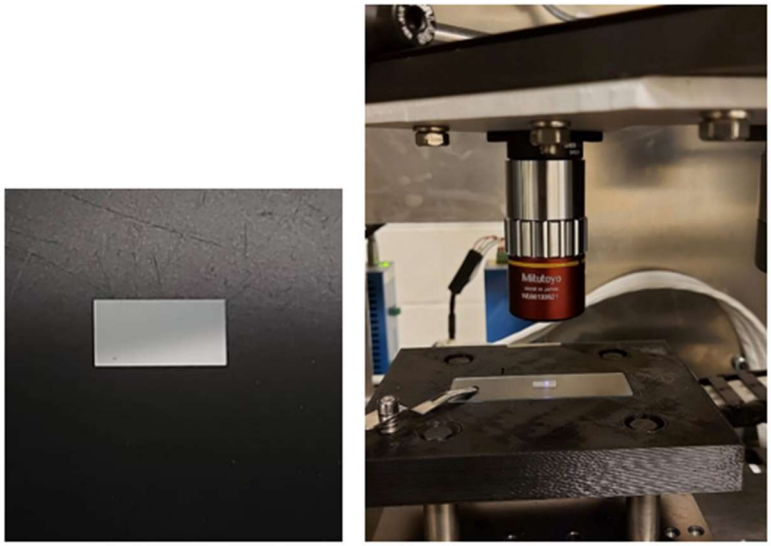

Figure 13: a) C plane sapphire wafer with dimensions of (10mmx5mmx0.5mm) b) Femtosecond laser writing on C plane sapphire wafer

Ultrashort femtosecond laser processing

The experimental setup, which includes a spectra physics femtosecond laser with a central wavelength of 1040nm, a pulse duration of 300fs, and a maximum pulse energy of 40uJ at 200KHZ, is depicted in Figure 14. Through a few mirrors and a lens (10X Mitutoyo Plan Apo NIR Infinity Corrected Objective Lens with a working distance of 30.5 mm), the laser incidence is modified into the surface of the samples set up in a 3D moving stage. By adjusting the values of X, Y, and Z after several runs and revisions, the surface of samples is identified. The surface of

samples is diagnosed after many runs and adjustments with the values of X, Y and Z. The X, Y, and Z axes were managed by a motion controller using G-code on three Aerotech stages. The focusing conditions and the laser parameters were different for glass of dimensions (10mmx5mmx1mm) and A&C plane sapphire crystals of dimensions (10mmx5mmx0.5mm). Still, the results of glass samples are used as reference while writing the pulse filamentation in the sapphire samples, thereby can avoid a lot of confusions.

Figure 15: Experimental setup for femtosecond laser processing

For the glass and sapphire samples, did lots of runs by varying the laser parameters and x, y, z values, and programmed to write many lines with change in x(dx) and z (dz) for constant value of y. In order calibrate the pulse spacing to 5um and spot size diameter to 10 um, the range of values for Pulse Picker Divider (PPD), Laser Energy and Feed Rate were calculated. Then started the

experiments by varying the laser parameters within the ranges calculated. There are like many sets of lines, with each set having 10 lines with different z pitch (dz) and dx. If the surface can be located right away, all of the lines can be inscribed inside the main body of glass; otherwise, some lines will be missed. The values of applied laser parameters and stage movements to scan glass samples are illustrated here, Table 1. The laser parameters and stage moving distances to write pulse filamentary voids in C & A planes of sapphire samples are described in the tables [2] and [3] respectively.

Table 1*: Laser parameters and stage movements applied for Glass*

Run No	LE (uJ)	PPD	Frequency (KHZ)	Scanning speed (mm/s)	Change in x, dx (um)	Change in z, dz (um)	Y value (mm)
1	16	2	100000	0.5	100	50	11
2	8	1	200000	0.1	100	50	11
3	12	1	200000	0.1	100	50	11
4	20	2	100000	0.25	100	50	11
5	32	2	100000	0.5	100	50	11

Table 2: Laser parameters and stage movements applied for C plane sapphire

Run	LE	PPD	Frequency	Scanning speed(mm/s)	Change in x, dx	Change in z, dz	Y value (mm)
1	5.6	1	200000	0.1	100	50	10
2	6.4	1	200000	0.2	100	50	10
3	7.2	1	200000	0.3	100	50	10
4	4	1	200000	0.2	30	25	10
5	2.4	1	200000	0.2	30	25	10
6	0.8	1	200000	0.2	100	50	10
7	2.4	1	200000	0.2	30	50	11
8	3.2	1	200000	0.2	30	50	11
9	2.4	2	100000	0.2	30	50	11
10	3.2	2	100000	0.2	30	50	11

Table 3: Laser parameters and stage movements applied for A plane sapphire

Run	LE	PPD	Frequency	Scanning speed(mm/s)	Change in x, dx	Change in z, dz	Y value (mm)
1	2.4	2	100000	0.2	30	25	10
2	4	2	100000	0.2	30	25	10
3	3.2	1	200000	0.2	30	40	10
4	3.2	2	200000	0.2	30	40	10
5	4.8	1	200000	0.3	30	50	11
6	5.6	1	200000	0.3	30	50	11
7	6.4	1	200000	0.3	30	50	11
8	0.8	1	200000	0.2	30	50	11
9	1.6	1	200000	0.2	30	50	11

Polishing

Sapphire wafers after writing refractive index variations need to cut in the middle in order to view the cross section for further analysis. As sapphire is very hard, while cutting with lasers and diamond cutter creates a lot of cracks, which makes it really difficult to view the pulse filamentary voids of refractive index variations. Thus, the cross sections must be polished in order to see the voids that cracks have obscured. For that, the samples are fossilized in the epoxy resin and allowed to cure for 24 hours. Remove the hardened epoxy along with submerged samples (Figure 11b) from the mold once it has cured out and polish the samples using silicon carbide grids

with numbers 120, 240, 600/P1200, and 800/P2400, respectively, and thereafter with fiber polishing kit (Figure 11a). The size of the abrasive particles in the polish grids decreases with the increase in its number. The size of abrasives is in the order of 106 um, 66 um, 12 um and 6 um for the numbers 120, 240, 600/P1200 and 800/P2400 respectively. The lapping films of fiber grids from left have particle sizes 5 um, 1 um and 0.3 um respectively.

Figure 12: a) Fiber Grids b) Polishes samples

Microscope analysis

The optical microscope (Figure 12), which has five different types of lenses for varying magnifications, was used to investigate each sample of glass and sapphire. The five different types of lenses are 5X, 10X, 20X, 50X, and 100X for the scales 500 um, 200 um, 100 um, 50 um, and 20 ums, respectively. The computer and microscope are linked so that LAZ EZ software can be used to produce better images. Depending on the characteristics of the samples, utilized two different cameras: 2) Basler camera with Pylon viewer software, and 1) Leica camera with LAZ EZ software.

Figure 13: a) Leica optical microscope with its own camera b) Basler camera

Optigrating simulation

Using the Opti grating software, first created a FBG in Sapphire optical fiber with core refractive index of 1.746. The sapphire optical fiber is having only core, as the cladding is air in the practical case, so the diameter of the core and cladding is kept as 125 and 500 ums respectively with refractive indices of 1.746 and 1.00 respectively. The central wavelength has chosen as 1.55 um. The radial and azimuthal photosensitivity are chosen as 1 for both cladding and core with a real profile for the fiber. I have created 10 LP m, n modes from m = 0 to 10 to create multimode sapphire optical fiber and selected all the modes with input amplitude and phase values set as 1 and 0 respectively. The length of the grating has kept as 10 mm and period of the grating as 0.879 um. The resultant FBG came up with a Bragg wavelength of 1.49 um. Then tried to see the relationship between Grating period and Bragg wavelength by creating different FBGs by varying the grating period. As per the equation, a linear relationship between Grating Period and Bragg Wavelength is seen, i.e., when the value of grating period increases, the Bragg peak shift towards right(increases)[42].

Secondly, did a simulation of a temperature sensor and checked the sensitivity by varying the temperature linearly in different temperature ranges. At uniform temperature of 25oC, the Bragg wavelength was at 1.549 um. The Bragg shift has been studied with temperature values ranging from 1400 ^{o}C to 2000 ^{o}C. As the temperature increases, Bragg wavelength shifted towards right (red shift) and as the temperature decreases, the Bragg wavelength shifted towards left (blue shift).

Thirdly, did a simulation of a strain sensor and checked the sensitivity by varying the strain linearly from -200 to 200. The parameters used in this case are as follows, core diameter = 60 um, Refractive index = 1.746, Length of the Grating = 5000um = 5mm, Grating Period = 1um. As per the strain applied, there showed a shift in the Bragg wavelength[43].

CHAPTER IV

RESULTS & DISCUSSIONS

Glass

The femtosecond laser experimental setup was used in numerous studies to process glass for diagnosing the optimal conditions. Finally, with the laser energy of 8uJ, feed rates of 0.1 and 0.2 mm/s, and a pulse picker divider of 1, satisfactory results were discovered. With the aforementioned laser settings and focused using a 10X infinity-corrected objective lens, controlled pulse filamentation was obtained with controlled damage. The distance between the two consecutive pulse filamentary voids in z axis is 50 um(z pitch), and in y axis (dx) is 100 um. The images of the cross sections before and after polishing are shown below [Figure 14 & 15] and it's clear that samples after polishing have improved a lot compared to before polishing samples as the pulse filamentation is clearly visible.

Before & after polishing:

In this case, it is possible to observe filament propagation through a glass medium, the filament lines look like having more width and also lines are not that straight due to the roughness of cross-section. When writing directly on glass using femtosecond laser, the glass is actually melted in a controlled manner and then rapidly solidified. In fact, deformation-based processes occur, and when the glass wafer is cut, changes occur suddenly that lead to cracks and damage.

Roughness results from sudden breakage of the glass with a laser cut or diamond cutter just after the glass has rapidly solidified. The beam radius of the fs laser is less when compared to the ns and ps lasers, there by the self-focusing effect will be higher because of Kerr effect. Here the self-

focusing can be clearly seen in following images of glass samples processed using 8uJ pulse energy. Figures [14] shows the images of glass samples before polishing., where we can see 12-15 pulse filamentary voids from top to bottom of the cross section obeying a diagonal pattern. The diagonal pattern is due to variations in the x and z values while scanning the sample, here change in x values (dx) is to create different lines along the surface of wafer and change in z values (dz) to create depth along the thickness of wafer. In comparison to the filaments before polishing, the lines inside the glass medium are straighter and leaner (smaller in diameter) after polishing. This demonstrates how polishing enhanced the cross-section surface by removing cracks and damage and improving the image. This can be proved from the following figure [15] of polished samples, which is processed with 8uJ pulse energy, and a feed rate of 0.2 mm/s with repetition rate 200KHZ. The length and width of the refractive index voids reduces as the depth (z) increases.

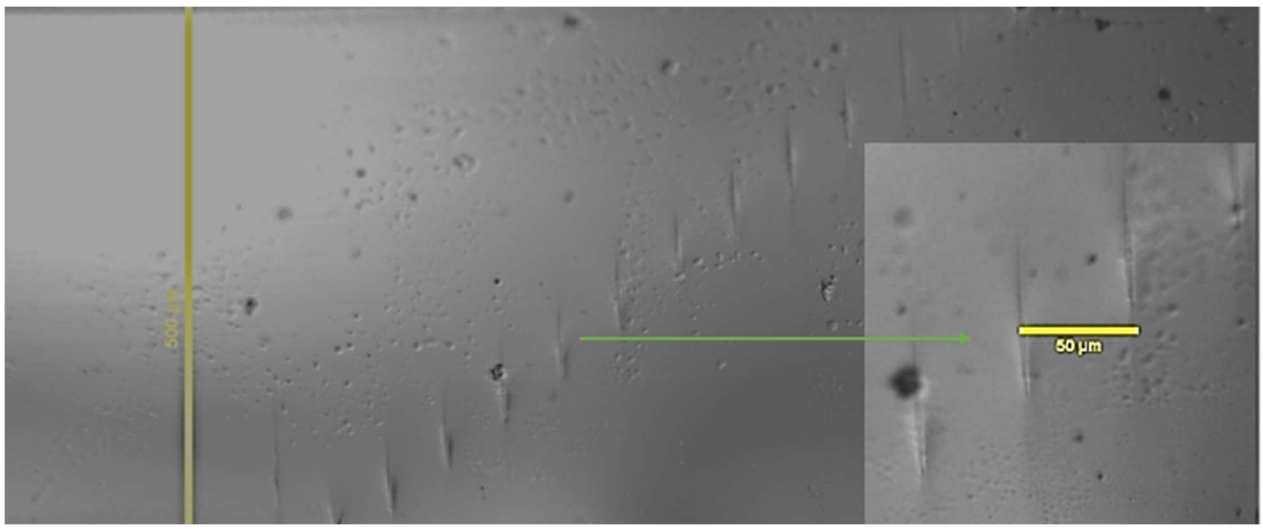

Figure 16: Pulse Filamentary Voids in Glass with pulse energy of 8uJ (before polishing)

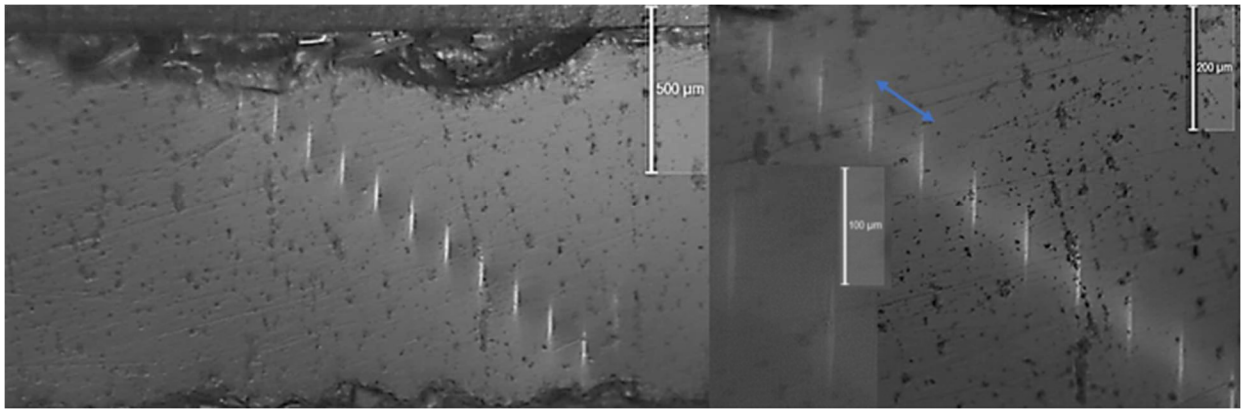

Figure 17: Pulse Filamentary Voids in Glass with pulse energy of 8uJ (after polishing)

The morphology of the refractive index voids mainly depends on the laser energy, which is shown in the figure [16] below. Pulse filamentation occurs only when the laser peak power is above the ionization threshold of the material. From the figure, its visible that the length and width of the pulse filaments increases with the increase in pulse energy, and then starts decreasing and finally saturates when the pulse energy go beyond a particular threshold. The length and breadth of corresponding pulse energies were calculated and drawn a graph to see the pattern of variation, which fits to the explanation that did above.

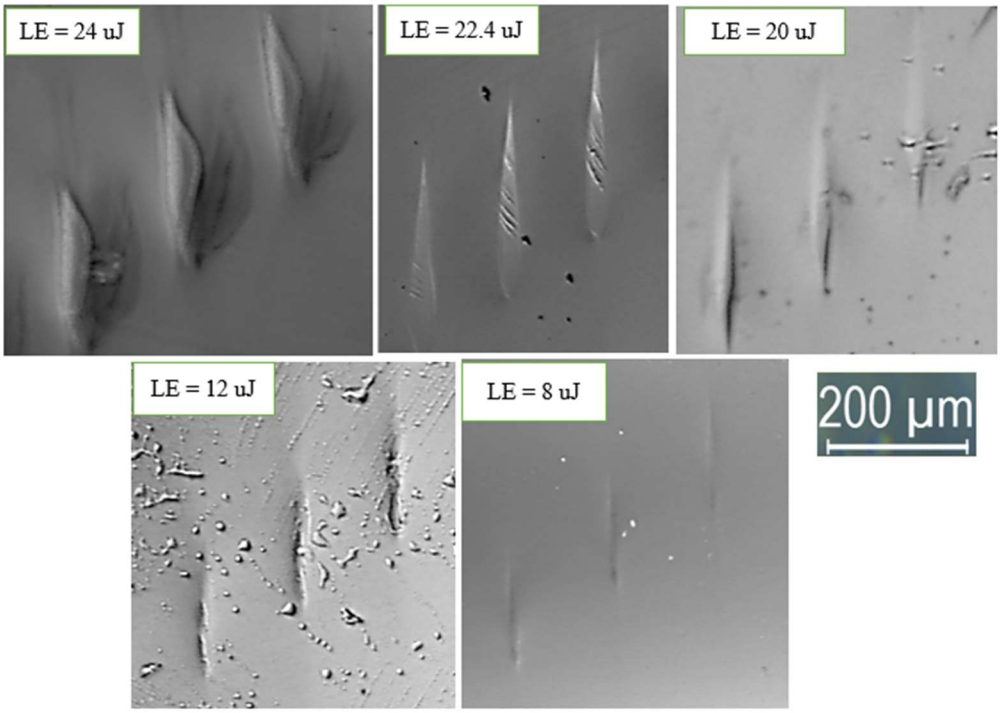

Figure 18: Variation in the morphology (Length & Width) of the pulse filamentary voids with pulse energy

The following table [4] shows the variations in length and width of the refractive index voids inside glass wafers corresponding to their laser energies at a particular depth in the cross-sections. For the lowest laser energy 8 uJ, got the smallest length and width, which is 169 um and 14 um respectively. When the laser energies increases until a threshold value, the length and breadth of the filaments also increases. After crossing the threshold limit of uncontrolled damages, the values of length and breadth starts decreasing and thereafter gets saturate. The highest length of the refractive index void happens for the pulse energy 22.4 uJ, and thereafter the morphological values start decreasing and thereafter saturating.

Table 4: Length and width of refractive index voids with rescpect to the laser energies

No:	Laser Energy (uJ)	Length of Pulse Filamentary Void(um)	Width of Pulse Filamentary Void(um)
1	24	234	50
2	22.4	258	48
3	20	281	30
4	12	181	18
5	8	169	14

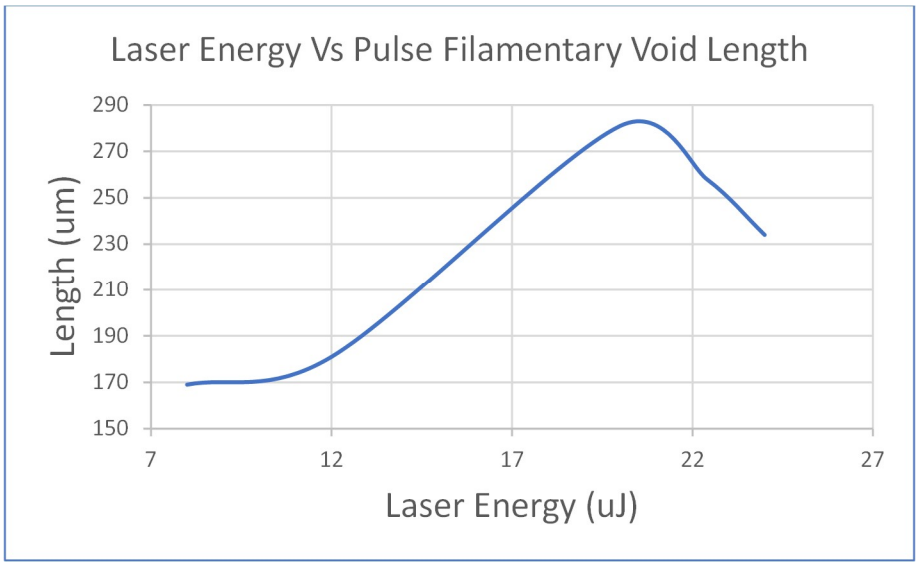

Figure 19: Graph of Laser Energy Vs Filamentary Void Length

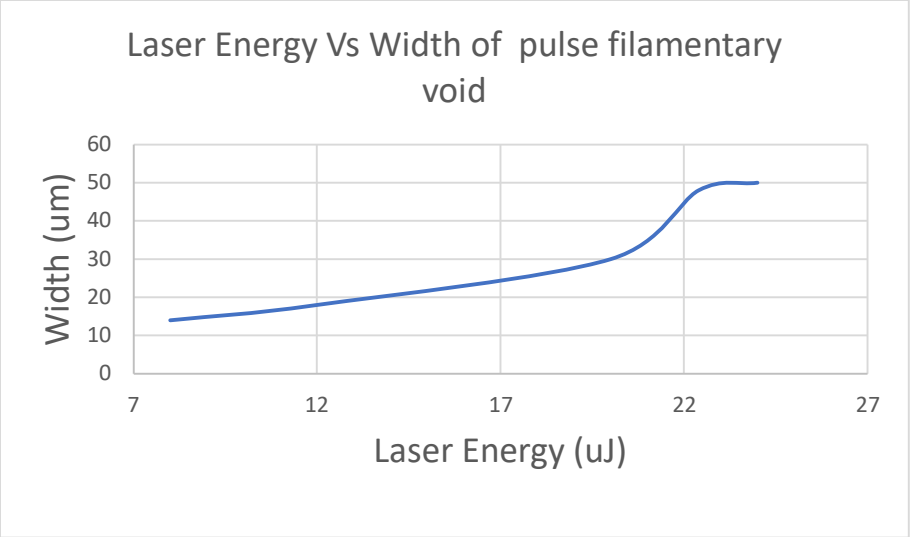

Figure 20:Graph of Laser Energy Vs Width of Pulse Filamentary Void

The upper graphs [Figs 17 and 18] highlight the previously discussed fact, namely the effect of laser energy on the morphology of the pulsed filament cavity generated by a femtosecond laser with a central wavelength of 1040 nm. The graph shows a tendency to initially increase in length and width as the laser power increases up to a certain threshold, then decreasing values and thereafter saturates when the laser power exceeds the threshold.

A plane sapphire

Numerous investigations have processed A plane sapphire using the femtosecond laser experimental setup while modifying the laser settings and focusing circumstances to obtain the ideal parameters. Finally, good results were found using laser energies in the range of 2-3.5 uJ, feed rates of 0.2 and 0.3 mm/s, and a pulse picker divider of 1. Pulse filamentation was achieved using the aforementioned laser settings and focussing with a 10X infinity-corrected objective lens, although the backdrop appears to be damaged with many cracks. The laser or diamond cutter

cutting causes the fissures to form. Coarse and fine polishing was used to get rid of these cracks, greatly improving the sample. The photos of A planar sapphire cross-sections in the figures below, before and after polishing, will give a clear idea of the changes. The difference in x value in each set of lines is 30 um, and there is a 50 um space between the two consecutive lines of high refractive index. There are five different sets of lines, each 60 um apart and fed at a slightly different rate and pulse energies. The wafer measures 10 millimeters in length, 5 millimeters in width, and 500 um in thickness. Below are images of the cross sections before and after polishing [Figures 19 & 20]. It is evident that samples after polishing have significantly improved compared to samples before polishing as the pulse filamentation is clearly visible.

Before and after polishing

Compared to glass, sapphire is too hard and brittle, especially A plane sapphire. Therefore, the controlled melting inside A plane sapphire can be attained with a laser energy value greater than the value for glass and lower than the value for C plane sapphire. Once ionization of sapphire is achieved with the triggered pulse energy, the material properties get changed and then re-solidifies back like a deformation process. After quick re-solidification, the sample material is prone to get damages with even a small perturbation. Therefore, A plane sapphire sample cross-section ended up in damages and cracks when it is exposed to a sudden cut by laser or diamond cutter. Because of the flaws and damage created during the wafer cutting process, the A plane sapphire treated samples look terrible when examined under a microscope. Due to its harsh and abrasive character, the pulse filamentation lines appear to be destroyed prior to polishing (Figure 19). Although the cross section obtained after the cutting is utterly unpolished and caused this ugly

picture, it does not imply that self-focusing did not occur at all, as evidenced by the photographs of polished samples. After polishing**,** A plane sapphire processed samples after polishing really give a hope, as the filaments are good looking, straight and with less width. This proves that, within the range of pulse energies “2.4 - 4 uJ”, can be managed to produce a nice pulse filamentation void inside the A sapphire wafer, which can be viewed in Figure 20.

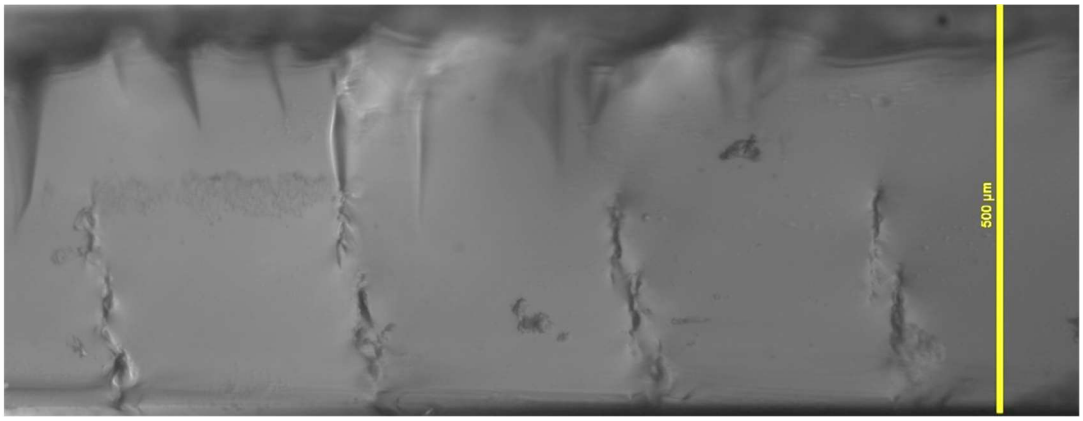

Figure 21: Filamentary Voids in A plane sapphire (before polishing)

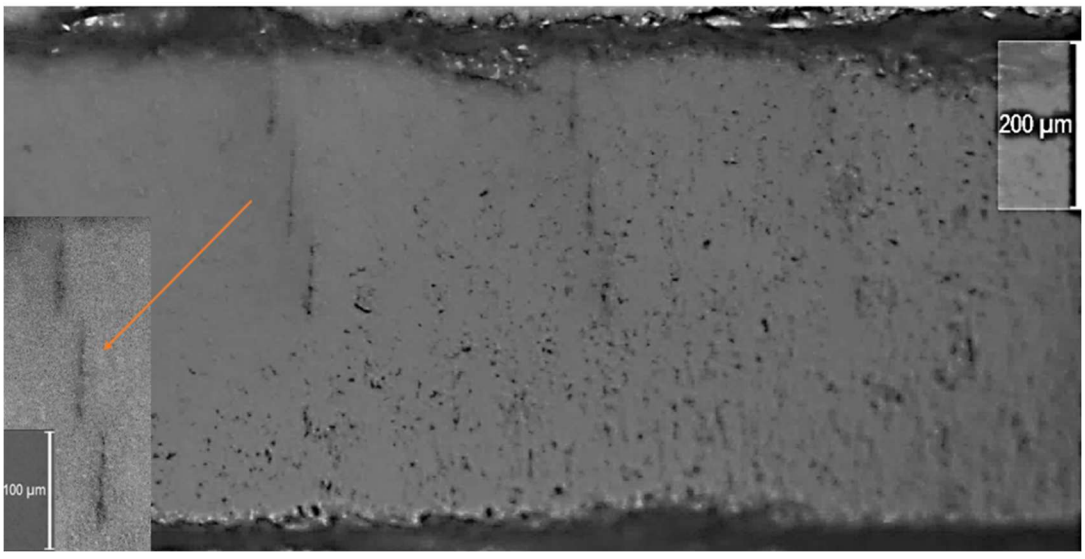

Figure 22: Filamentary Voids in A plane sapphire (after polishing)

With increasing laser energy, the filamentary voids in sapphire in A plane get longer. The filament length grows with an increase in pulse energy within the controlled ionization pulse energy. However, once the laser intensity goes above the threshold limit, the length of the refractive index voids starts to decrease and eventually reaches saturation. This is due to the fact that diffraction and plasma defocusing completely replace and dominate the self-focusing effect, resulting in filament termination. The graph below [Figure 21] shows the tendancy of A plane sapphire to change its morphology with respect to the pulse energy.

Table 5: Variation of Filamentary Length with Pulse Energy

Laser Energy(uJ)	Length (um)
3.2	51
4	74
4.8	78
5.6	106
6.4	121

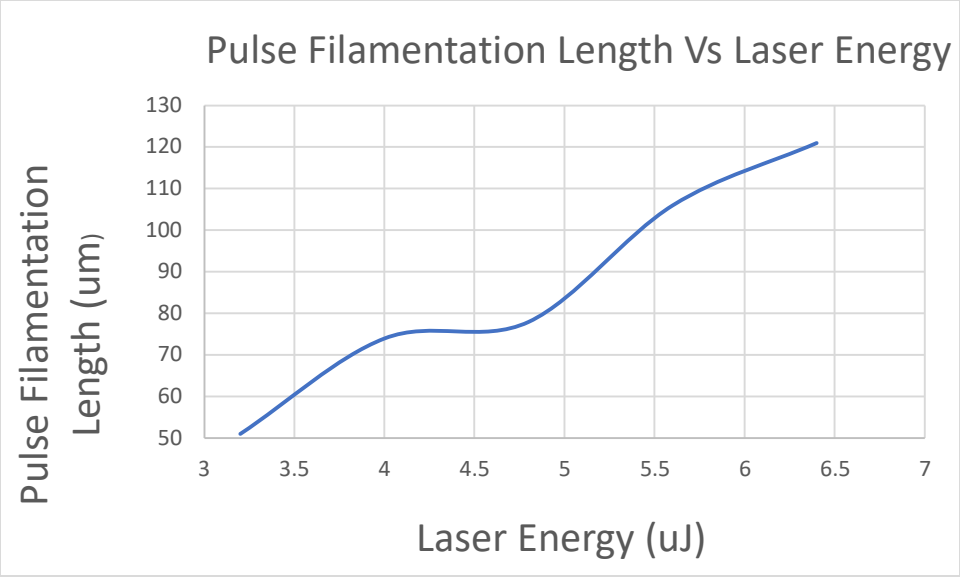

Figure 23: Dependence of Pulse Filamentation Length with Pulse Energy

C plane sapphire

Numerous investigations have processed C plane sapphire using the femtosecond laser experimental setup while modifying the laser settings and focusing circumstances to obtain the ideal parameters. Finally, good results were found using laser energies 1.6 & 2.4 uJ, feed rate of 0.2 mm/s, and a pulse picker divider of 1. Pulse filamentation was achieved using the aforementioned laser settings and focussing with a 10X infinity-corrected objective lens, although the backdrop appears to be damaged with a few cracks. The laser or diamond cutter cutting causes the fissures to form. Coarse and fine polishing was used to get rid of these cracks, greatly improving the sample. The photos of C planar sapphire cross-sections in the figures below, before and after polishing, will give a clear idea of the changes. Below are images of the cross sections

before and after polishing [Figure 21 & 22]. It is evident that samples after polishing have significantly improved compared to samples before polishing as the pulse filamentation is clearly visible.

Before & after polish

The C plane sapphire processed samples before polishing [Figure 22] looks better than A plane sapphire, but still got a few cracks and filaments produced by 2.5 uJ looks like a bit damaged. This damage look doesn't mean that the lines are not self-focused or damaged instead of producing refractive index variations, but because of the hardness nature of sapphire. This can be understood from the images of polished samples. The polished C plane sapphire processed samples seems far better than the unpolished ones, which emphasis the hardness nature of sapphire wafers. From the beautiful filaments, its proved that refractive index variations can be controlled using pulse energies of 1.5 & 2.5 uJ inside the medium of C plane sapphire. This can be seen in the following figures [Figure 22 & 23] of polished samples.

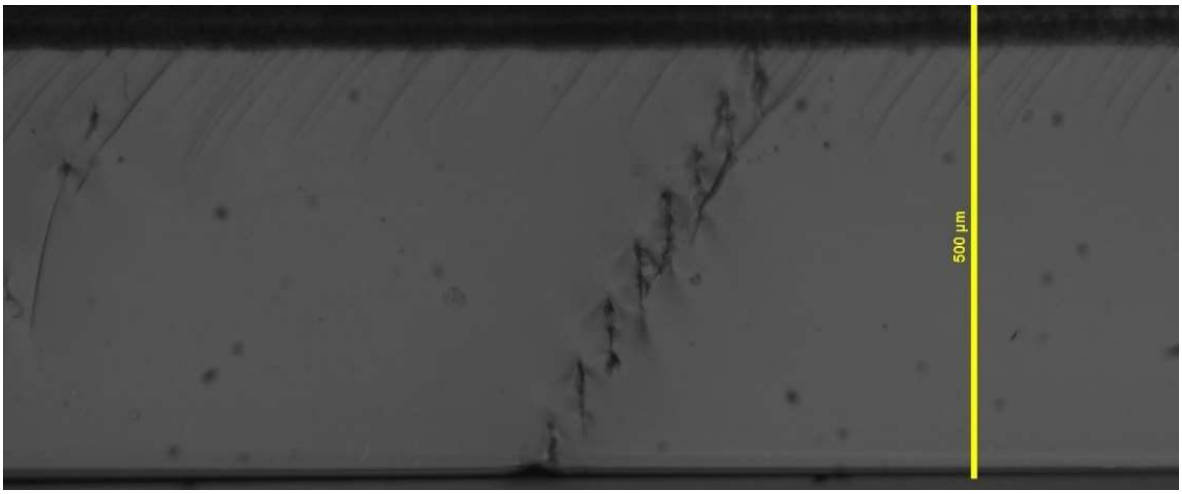

Figure 24: Pulse Filamentation in C plane sapphire (before polishing)

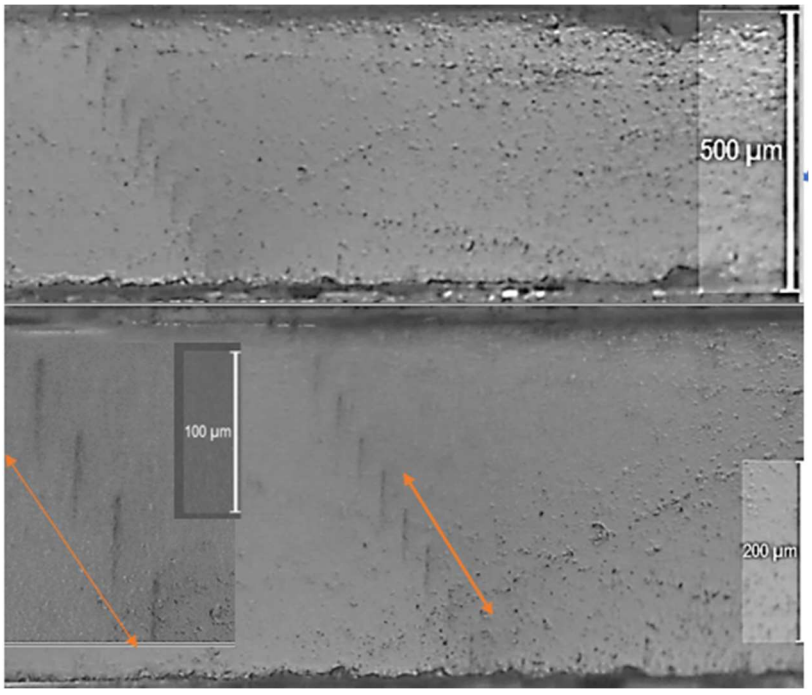

Figure 25: Pulse Filamentation in C plane sapphire (after polishing)

When the pulse energy is increased within a specified damage threshold, the length of the refractive index voids has a tendency to lengthen. Beyond the threshold limit, the length of voids

first shorten before becoming saturated as the pulse filamentary line stops, when the Kerr effect's self-focusing is overcome or largely replaced by plasma defocusing and diffraction. Due to the decreased power of all the studies, the width has very little effect on the outcomes. Also, there is a tendancy for the filaments to increase or decrease in length as the thicknes of the crossesection varies (dz) along the crosssection. This diagonal pattern of lines is due to change in the values of x (dx) along the surface and change in values of z (pitch) alongth the thickness.

.

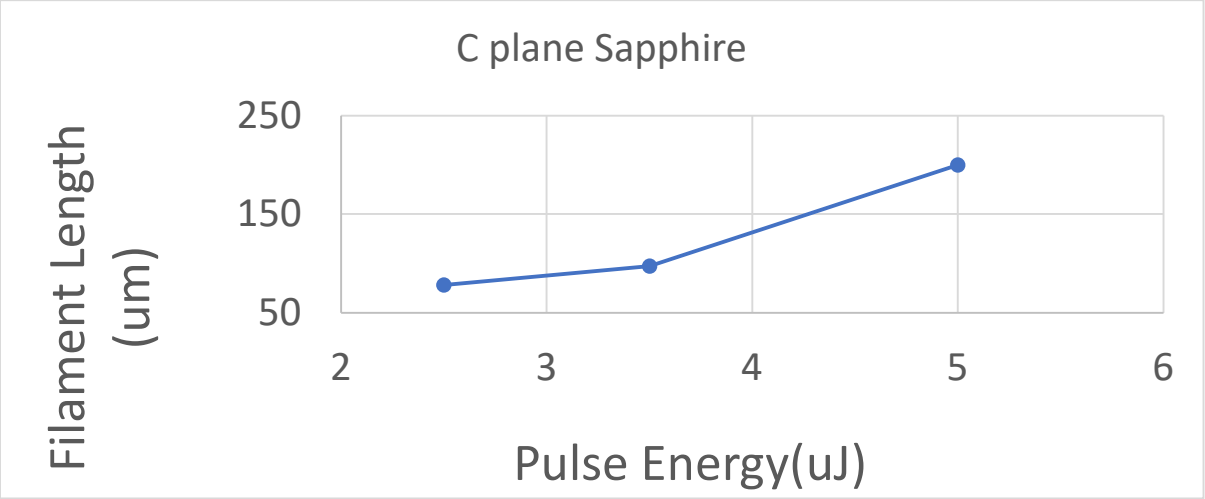

Figure 26: Relationship between pulse energy and pulse filamentation void in C plane

Simulation of FBGs in sapphire optical fiber

A Sapphire Fiber Bragg Grating is simulated and studied the reflection spectrum using the Opti grating software. The is formed at a wavelength of 1.49 um with a reflectivity of -3.060432e^{-001}dB. As a result of the peak's extreme pointiness, it is dominating because only one specific

wavelength is reflected, as opposed to a range of values that would not produce a pointed peak. The Forward Width Half Wave Maximum (FHWM) will be higher if the spectral response has a non-pointed peak, which implies that instead of having a specific reflected wavelength, there will be a range of wavelengths, which will result in poor sensing. The main challenge in fabricating a FBG is to get a prominent peak in the reflection spectra with low FWHM and high reflectivity.

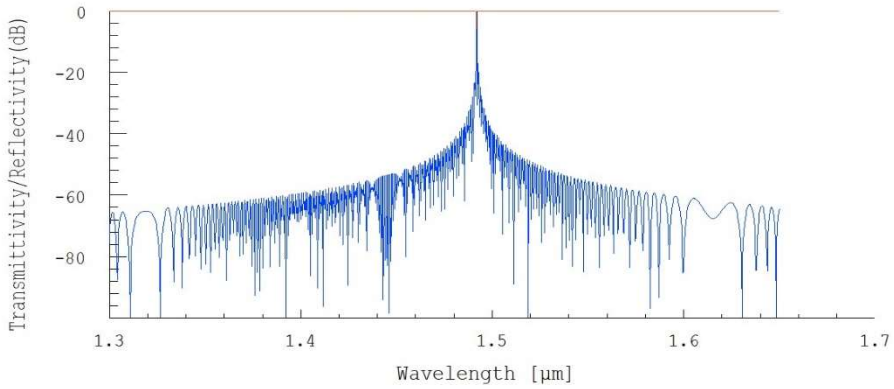

Figure 27: Transmittivity/Reflectivity Vs Bragg Wavelength of a simulated sapphire Fiber Bragg Grating

The relationship between Grating Period & Bragg Wavelength is studied by simulating different FBGs which satisfies the conditions for a standard FBG, with different grating period. As per the equation, a linear relationship between Grating Period and Bragg Wavelength is seen, i.e., when the value of grating period increases, the Bragg peak shift towards right (increases). The grating period should not go below or above the limited value, as per the equation.

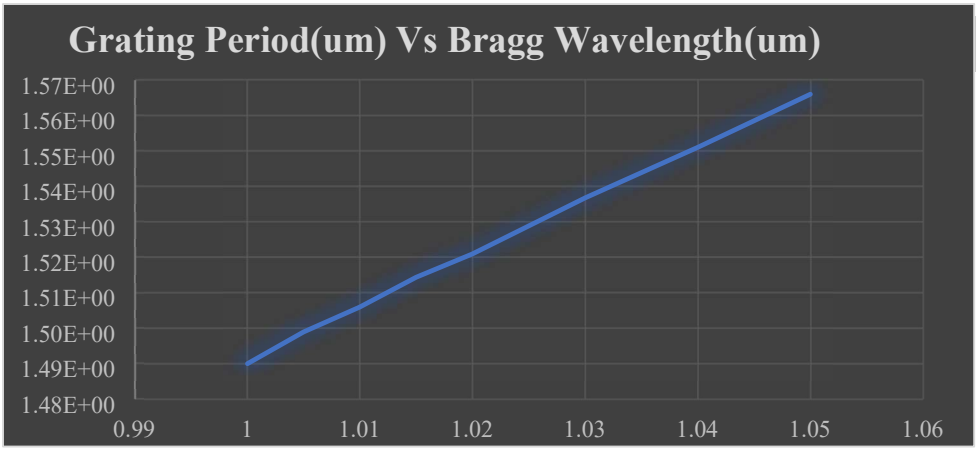

Figure 28: Relationship between Grating Period & Bragg wavelength.

Simulation of a sapphire fiber Bragg grating temperature sensor

A temperature sensor is simulated and checked the sensitivity by varying the temperature linearly in different temperature ranges. At uniform temperature of 25oC, the Bragg wavelength was at 1.549 um. The Bragg shift has been studied for various temperature sensors by varying the temperatures between 1400 _ 2000 ºC. As the temperature increases, Bragg wavelength shifted towards right (red shift) and as the temperature decreases, the Bragg wavelength shifted towards left (blue shift). The reflected peak here is not dominated as it is wide instead of pointed with high FWHM is high with low reflectivity. Need to work more on this simulation until we get a good reflection spectrum.

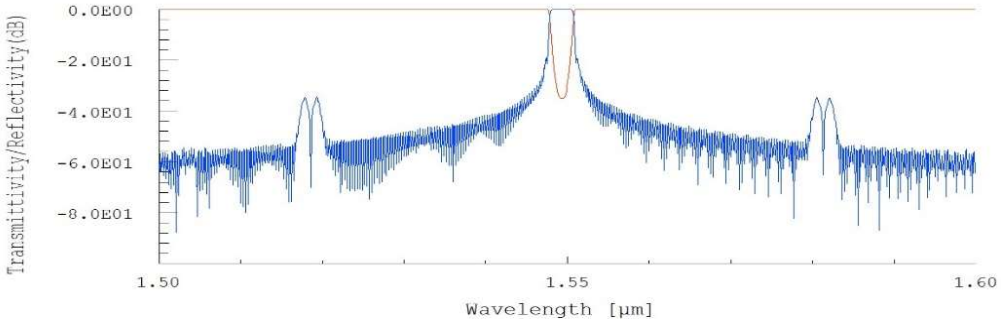

Figure 29: Transmittivity/Reflectivity Vs Bragg Wavelength of a simulated sapphire Fiber Bragg Grating temperature sensor.

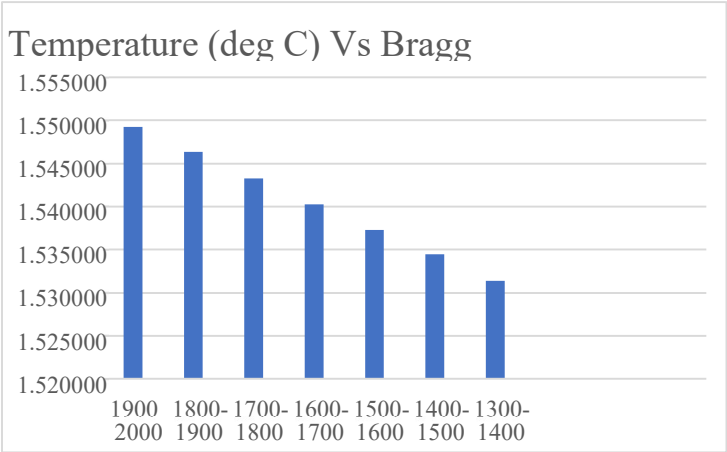

Figure 30: Temperature Vs Bragg Wavelength of different temperature sensors

Simulation of a sapphire fiber Bragg grating strain sensor

A strain sensor is simulated and checked the sensitivity by varying the strain linearly from -200 to 200. The parameters used in this case are as follows, core diameter = 60 um, Refractive index = 1.746, Length of the Grating = 5000um = 5mm, Grating Period = 1um. As per the strain applied, there showed a shift in the Bragg wavelength. Compared to temperature sensor, the strain

sensors here are having good spectra with pointed dominant wavelengths peak with low values of FWHM. The reflectivity is also high compared to the temperature sensor which will result in a better sensing. These parameters and dimensions can be followed while fabricating a physical sapphire strain fiber sensor to acquire a standard FBG with controlled damage and periodic morphology.

For Uniform strain:

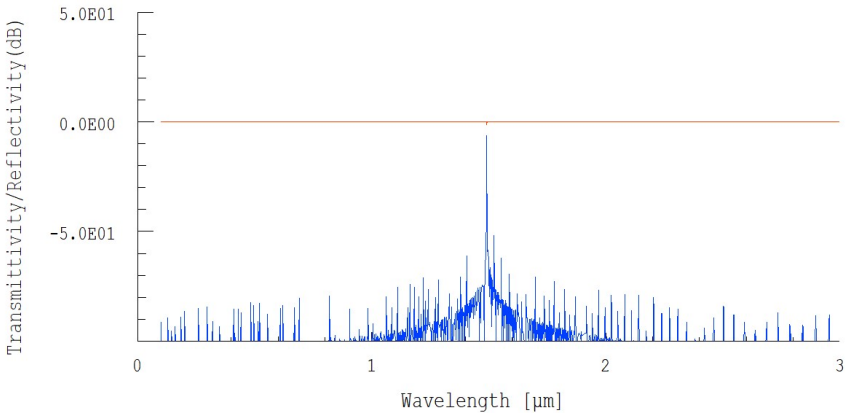

Figure 31: Transmittivity/Reflectivity Vs Bragg Wavelength of a simulated sapphire Fiber Bragg Grating strain sensor for uniform strain.

For Linear strain:

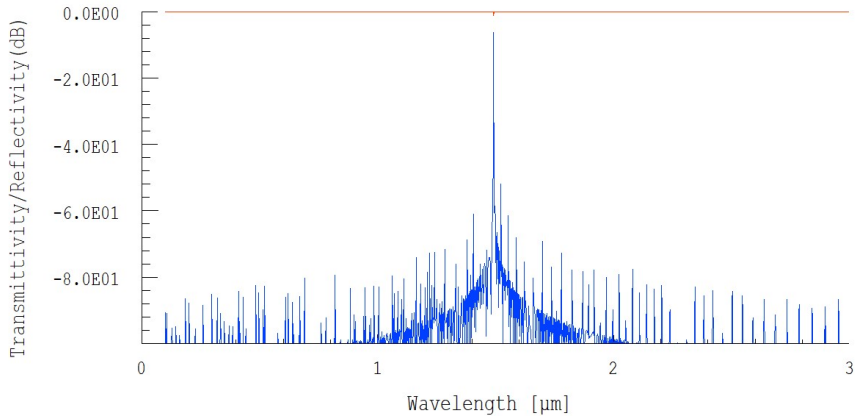

Figure 32: Transmittivity/Reflectivity Vs Bragg Wavelength of a simulated sapphire Fiber Bragg Grating strain sensor for linear strain.

CHAPTER V

CONCLUSIONS & FUTURE WORKS

Conclusions

Different runs of tests were used to adjust the laser settings and laser focusing conditions for the ultrashort processing of glass, sapphire A plane, and sapphire C plane. With feed rates of 0.1 and 0.2, a pulse picker divider of 1, and pulse energy of 8uJ, it can acquire pulse filamentation on glass. A 10X Mitutoyo Plan Apo NIR Infinity Corrected Objective Lens with a working distance of 30.5 mm is utilized for controlled focusing. The refractive index variations attained through the pulse filamentation can be make use of in the fabrication of Fiber Bragg Grating (FBG) optical fiber sensors, where the main problem is the creation of periodic refractive index variations. In conclusion, the aforementioned laser settings and the focusing circumstances on glass can be used to control the periodicity of refractive index fluctuations, resulting in effective FBGs[44][45].

Using an ultra-short, pulsed femtosecond laser, the processing conditions of C plane sapphire were able to be optimized after numerous rounds of tests with various laser settings and focusing conditions. Better pulse filamentation was achieved utilizing pulse energies of 1.5 and 2.5 uJ, a feed rate of 0.2 mm/s, a pulse picker divider of 1, and focusing with a 10X Mitutoyo Plan Apo NIR Infinity Corrected Objective Lens at a working distance of 30.5 mm. The processed wafers were split down the middle to see the cross sections in order to analyze the pulse filamentation lines within the sapphire. The slicing caused numerous cracks and other defects inside the wafer, making examination very challenging. This was overcome by employing optical fiber grids to polish the processed samples after cutting, which improved the samples.

In comparison to C plane sapphire, A plane sapphire is much harder and more abrasive, making processing it much more challenging. A planar sapphire is regarded as a subpar material for many device applications due of its processing challenges. A new way of thinking about A planar sapphire was made possible by this study's ability to tune the laser parameters and focusing conditions for processing the material. With A plane sapphire, this will open up a wide range of possibilities, including photonics device applications. The following laser settings and focusing circumstances are used to maximize the processing of a planar sapphire. A 10X Mitutoyo Plan Apo NIR Infinity Corrected Objective Lens was used to focus at a working distance of 30.5 mm with a laser energy between 2 and 3.5 uJ, feed rates between 0.2 and 0.3 mm/s, and a pulse picker divider of 1. To get satisfactory results for A plane sapphire, the cut samples must be polished

Future works

The polishing has improved the processed samples' quality, particularly the A plane sapphire. Finding the ideal polishing conditions for each sample (A & C plane sapphire) will greatly expand the possibilities for pulse filamentation and, in turn, for FBG sensors. In order to make sapphire viable for sensing applications in severe environments, better optimization is therefore required for both the A and C planes of sapphire. FBG simulations have already been performed using optigrating to optimize the length and period of the grating required to write FBG in sapphire optical fibers with a 60-um diameter and resultant sensor will operate at 1.5 um central wavelength. The objective of the upcoming work is to produce sapphire optical fiber sensors in challenging situations using optimal laser parameters, focusing circumstances, and simulation findings from sapphire wafer processing and Optigrating software, respectively

REFERENCES

[1] Fidanboylu and H. S. Efendioglu, “Fiber optic sensors and their applications,” *Symposium A Quarterly Journal In Modern Foreign Literatures*. pp. 1–6, 2009. [Online]. Available: http://iats09.karabuk.edu.tr/press/pro/02_KeynoteAddress.pdf

[2] P. Khandelwal, “Optical Fiber Sensors: Classification & Applications,” vol. II, no. Vii, pp. 22–25, 2013, [Online]. Available: www.ijltemas.in

[3] P. M. J, “A Survey Paper f Optical Fiber Sensor,” pp. 33–39.

[4] “Sensing with femtosecond laser filamentation.pdf.”

[5] T. Yan, L. Ji, and W. Sun, “Characteristics and formation mechanism of filamentary plasma string induced by single picosecond laser pulse in sapphire,” *Applied Physics A: Materials Science and Processing*, vol. 128, no. 1. 2022. doi: 10.1007/s00339-021-05147-8.

[6] Amina, L. F. Ji, T. Y. Yan, and R. Ma, “Ionization behavior and dynamics of picosecond laser filamentation in sapphire,” *Opto-Electronic Advances*, vol. 2, no. 8. pp. 1–7, 2019. doi: 10.29026/oea.2019.190003.

[7] T. Wu, Z. Wu, Y. He, Z. Zhu, L. Wang, and K. Yin, “Femtosecond laser textured porous nanowire structured glass for enhanced thermal imaging,” *Chinese Optics Letters*, vol. 20, no. 3. p. 033801, 2022. doi: 10.3788/col202220.033801.

[8] “FS laser induced refractive index modifications in fluoride glass.pdf.”

[9] G. Chen and J. Qiao, “Femtosecond-laser-enabled simultaneous figuring and finishing of glass with a subnanometer optical surface,” *Optics Letters*, vol. 47, no. 15. p. 3860, 2022. doi: 10.1364/ol.467413.

[10] J. Qiu, K. Miura, and K. Hirao, “Femtosecond laser-induced microfeatures in glasses and their applications,” *J. Non. Cryst. Solids*, vol. 354, no. 12–13, pp. 1100–1111, 2008, doi: 10.1016/j.jnoncrysol.2007.02.092.

[11] C. B. Schaffer, A. Brodeur, and E. Mazur, “Laser-induced breakdown and damage in bulk transparent materials induced by tightly focused femtosecond laser pulses,” *Meas. Sci. Technol.*, vol. 12, no. 11, pp. 1784–1794, 2001, doi: 10.1088/0957-0233/12/11/305.

[12] K. Itoh, W. Watanabe, S. Nolte, and C. B. Schaffer, “Ultrafast processes for bulk modification of transparent materials,” *MRS Bulletin*, vol. 31, no. 8. pp. 620–625, 2006. doi: 10.1557/mrs2006.159.

[13] F. Leplingard *et al.*, “FWM-Assisted Raman Laser for Second-Order Raman Pumping,” *Optics InfoBase Conference Papers*. pp. 431–432, 2003.

[14] M. Lancry, B. Poumellec, A. Chahid-Erraji, M. Beresna, and P. G. Kazansky, “Dependence of the femtosecond laser refractive index change thresholds on the chemical composition of doped-silica glasses,” *Optical Materials Express*, vol. 1, no. 4. p. 711, 2011. doi: 10.1364/ome.1.000711.

[15] “Free control of filaments rotating by vortex fs laser beams intereference in fused silica.pdf.”

[16] A. Butkutė and L. Jonušauskas, “3D Manufacturing of Glass Microstructures Using Femtosecond Laser,” *Micromachines*, vol. 12, no. 5. 2021. doi: 10.3390/mi12050499.
[17] Y. Shimotsuma, P. G. Kazansky, J. Qiu, and K. Hirao, “Self-organized nanogratings in glass irradiated by ultrashort light pulses,” *Phys. Rev. Lett.*, vol. 91, no. 24, p. 247405, Dec. 2003, doi: 10.1103/PHYSREVLETT.91.247405/FIGURES/3/MEDIUM.
[18] “Multiple pulse laser induced breakdown spectroscopy for monitoring the fs laser micromachining process of glass.pdf.”
[19] T. Liu, H. Wei, J. Wu, J. Lu, and Y. Zhang, “Modulation of crack formation inside single-crystal sapphire using ultrafast laser Bessel beams,” *Optics and Laser Technology*, vol. 136. 2021. doi: 10.1016/j.optlastec.2020.106778.
[20] T. Yan, L. Ji, R. Ma, Amina, and Z. Lin, “Modification characteristics of filamentary traces induced by loosely focused picosecond laser in sapphire,” *Ceramics International*, vol. 46, no. 10. pp. 16074–16079, 2020. doi: 10.1016/j.ceramint.2020.03.159.
[21] “Thermal and optical properties of the fs laser structured and stress induced birefringent regions in sapphire.pdf.”
[22] G. Ren, Y. Ito, H. Sun, and N. Sugita, “Temporal-spatial characteristics of filament induced by a femtosecond laser pulse in transparent dielectrics,” *Optics Express*, vol. 30, no. 4. p. 4954, 2022. doi: 10.1364/oe.449874.
[23] G. Eberle, M. Schmidt, F. Pude, and K. Wegener, “Laser surface and subsurface modification of sapphire using femtosecond pulses,” *Applied Surface Science*, vol. 378. pp. 504–512, 2016. doi: 10.1016/j.apsusc.2016.04.032.
[24] S. Juodkazis, K. Nishimura, and H. Misawa, “In-bulk and surface structuring of sapphire by femtosecond pulses,” *Applied Surface Science*, vol. 253, no. 15. pp. 6539–6544, 2007. doi: 10.1016/j.apsusc.2007.01.097.
[25] H. Jo, Y. Ito, J. Hattori, K. Nagato, and N. Sugita, “High-speed observation of damage generation during ultrashort pulse laser drilling of sapphire,” *Optics Communications*, vol. 495. 2021. doi: 10.1016/j.optcom.2021.127122.
[26] Amina, L. Ji, T. Yan, Y. Wang, and L. Li, “Characteristics of 1064 nm picosecond laser induced filamentary tracks and damages in sapphire,” *Optics and Laser Technology*, vol. 116. pp. 232–238, 2019. doi: 10.1016/j.optlastec.2019.03.019.
[27] “Anisotropy of material removal during laser induced plasma assisted ablation of sapphire.pdf.”
[28] “Manufacturing of Porous Glass by Femtosecond Laser Welding.pdf.”
[29] L. Cao *et al.*, “Study on the influence of sapphire crystal orientation on its chemical mechanical polishing,” *Applied Sciences (Switzerland)*, vol. 10, no. 22. pp. 1–10, 2020. doi: 10.3390/app10228065.
[30] K. Wang *et al.*, “Study on mechanism of crack propagation of sapphire single crystals of four different orientations under impact load and static load,” *Ceramics International*, vol. 45, no. 6. pp. 7359–7375, 2019. doi: 10.1016/j.ceramint.2019.01.021.
[31] B. Poumellec, M. Lancry, A. Chahid-Erraji, and P. G. Kazansky, “Modification thresholds in femtosecond laser processing of pure silica: review of dependencies on laser parameters

[Invited]," *Opt. Mater. Express*, vol. 1, no. 4, p. 766, 2011, doi: 10.1364/ome.1.000766.
[32] K. Mishchik *et al.*, "Nanosize structural modifications with polarization functions in ultrafast laser irradiated bulk fused silica," *Opt. Express*, vol. 18, no. 24, p. 24809, 2010, doi: 10.1364/oe.18.024809.
[33] P. Lu, D. Grobnic, and S. J. Mihailov, "Characterization of the birefringence in fiber Bragg gratings fabricated with an ultrafast-infrared laser," *J. Light. Technol.*, vol. 25, no. 3, pp. 779–786, 2007, doi: 10.1109/JLT.2006.889662.
[34] C. W. Smelser, S. J. Mihailov, and D. Grobnic, "Formation of Type I-IR and Type II-IR gratings with an ultrafast IR laser and a phase mask," *Opt. Express*, vol. 13, no. 14, p. 5377, 2005, doi: 10.1364/opex.13.005377.
[35] E. N. Glezer and E. Mazur, "Ultrafast-laser driven micro-explosions in transparent materials," *Appl. Phys. Lett.*, vol. 71, no. 7, pp. 882–884, 1997, doi: 10.1063/1.119677.
[36] S. M. Eaton *et al.*, "Heat accumulation effects in femtosecond laser-written waveguides with variable repetition rate," *Opt. Express*, vol. 13, no. 12, p. 4708, 2005, doi: 10.1364/opex.13.004708.
[37] S. M. Eaton *et al.*, "Transition from thermal diffusion to heat accumulation in high repetition rate femtosecond laser writing of buried optical waveguides," *Opt. Express*, vol. 16, no. 13, p. 9443, 2008, doi: 10.1364/oe.16.009443.
[38] S. Richter *et al.*, "The role of self-trapped excitons and defects in the formation of nanogratings in fused silica," *Opt. Lett.*, vol. 37, no. 4, p. 482, 2012, doi: 10.1364/ol.37.000482.
[39] S. Richter, M. Heinrich, S. Döring, A. Tünnermann, and S. Nolte, "Formation of femtosecond laser-induced nanogratings at high repetition rates," *Appl. Phys. A Mater. Sci. Process.*, vol. 104, no. 2, pp. 503–507, 2011, doi: 10.1007/s00339-011-6489-7.
[40] Q. Wen, P. Zhang, G. Cheng, F. Jiang, and X. Lu, "Crystalline orientation effects on material removal of sapphire by femtosecond laser irradiation," *Ceramics International*, vol. 45, no. 17. pp. 23501–23508, 2019. doi: 10.1016/j.ceramint.2019.08.056.
[41] Q. Wen *et al.*, "Crystal orientation-dependent scribing of A-, C-, and M-plane sapphires by an ultraviolet laser," *Ceramics International*, vol. 48, no. 13. pp. 18842–18854, 2022. doi: 10.1016/j.ceramint.2022.03.161.
[42] M. M. A. Eid and A. N. Z. Rashed, "Numerical simulation of long-period grating sensors (LPGS) transmission spectrum behavior under strain and temperature effects," *Sens. Rev.*, vol. 41, no. 2, pp. 192–199, 2021, doi: 10.1108/SR-10-2020-0248/FULL/PDF.
[43] M. M. Elgaud, M. S. D. Zan, A. A. G. Abushagur, and A. A. A. Bakar, "Analysis of independent strain-temperature fiber Bragg grating sensing technique using OptiSystem and OptiGrating," *2016 IEEE 6th Int. Conf. Photonics, ICP 2016*, Jul. 2016, doi: 10.1109/ICP.2016.7510036.
[44] "Photonic circuits written by femtosecond laser in glass.pdf."

APPENDIX

APPENDIX

DEFINITIONS

FBG (Fiber Bragg Grating) - A fiber Bragg grating (FBG) is a type of distributed Bragg reflector that is built into a short segment of optical fiber and reflects specific wavelengths while transmitting all others. This is accomplished by generating a wavelength-specific dielectric mirror by creating a periodic variation in the refractive index of the fiber core. As a result, a fiber Bragg grating can be used as an inline optical fiber to block specific wavelengths, for sensing applications,[1] or as a wavelength- specific reflector.

OPTICAL FIBER - Optical fiber is a data transmission technology that uses light pulses that travel along a long fiber that is typically made of plastic or glass. Metal wires are preferred for optical fiber communication transmission because signals travel with less damage. Electromagnetic interference has no effect on optical fibers. The fiber optical cable employs total internal reflection of light. The fibers are designed in such a way that light can propagate along with the optical fiber depending on the power and distance of transmission required. For long-distance transmission, single-mode fiber is used, while multimode fiber is used for shorter distances. These fibers' outer cladding requires more protection than metal wires.

BIOGRAPHICAL SKETCH

Anitha earned her B.S. Physics degree from the University of Calicut, Kerala, India followed by a MS in Photonics from National Institute of Technology Calicut, Kerala, India. During the MS in Photonics, she was able to do research in the field of Nonlinear Optics and did an internship in the field of Langmuir thin films and its sensing applications at Raman Research Institute, Bangalore, India. After her first MS, she worked in the field of Photonic Crystals & Hydrogen Storage at the Indian Institute of Technology Madras, India for 2.5 years. Her passion towards studies made her to migrate to United States in August 2018 and graduated with MS in Interdisciplinary Science & Technology in May 2020 & MS in Manufacturing Engineering in December 2022 from the University of Texas, Rio Grande Valley (UTRGV).

Anitha worked as a Research Assistant at UTRGV while pursuing her MS in Manufacturing Engineering, where she researched in "Ultrafast Laser Induced Index Modifications in Dielectrics for Sensing Applications." She created Fiber Bragg Gratings (FBG) in sapphire optical fiber for harsh-environment sensing applications. UTRGV selected her as a Profiles in Excellence in 2021, and she received the Sustainability Fellowship during her master's degree in manufacturing engineering. She can be reached at anithan2020@gmail.com.